Journal of
Synchrotron
Radiation

ISSN 0909-0495

Received 5 March 2009
Accepted 26 June 2009

The coherency of synchrotron radiation at Pohang Accelerator Laboratory

Yong Woon Parc,[a] Changbum Kim,[b] Jung Yun Huang[b] and In Soo Ko[a]*

[a]Department of Physics, Pohang University of Science and Technology, Pohang 790-784, Republic of Korea, and [b]Pohang Accelerator Laboratory, Pohang University of Science and Technology, Pohang 790-784, Republic of Korea. E-mail: isko@postech.ac.kr

The coherency of the synchrotron radiation at Pohang Accelerator Laboratory has been investigated using Young's interferometer. The electron beam size can be measured precisely using the interferometer. An interferogram using 650 nm light at the diagnostics beamline at Pohang Light Source (PLS) has been measured to determine the electron beam distribution and the spatial coherence length. Interferograms obtained by numerical study are compared with experimental results in order to understand the measured data. From this comparison, the electron beam at PLS is revealed to be a Gaussian distribution with a standard deviation of 210 μm. The spatial coherency length of 650 nm light at PLS is measured to be 0.57 cm, and that of 0.1 nm light at PLS is predicted to be 0.88 μm by the same numerical study.

Keywords: coherence; interference; light source size.

1. Introduction

During the past several decades, interferometer techniques have been successfully implemented to measure the size of the light source at various storage rings (Mitsuhashi, 1999; Flanagan *et al.*, 2000; Fisher *et al.*, 2001; Sakai *et al.*, 2000; Masaki & Takano, 2003). Recently, numerical and experimental studies have been carried out to improve the measurement techniques (Naito & Mitsuhashi, 2006). Pohang Accelerator Laboratory (PAL) was founded in 1988 at Pohang University of Science and Technology (POSTECH) in Korea. Pohang Light Source (PLS), constructed at PAL, is a synchrotron radiation facility with a 2.5 GeV electron beam.

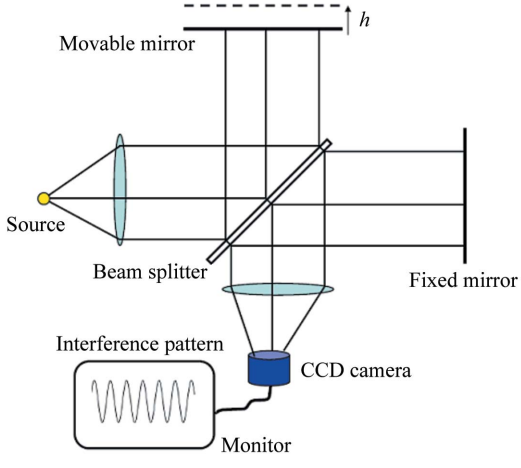

Figure 1
Michelson interferometer. h is the moving distance of the movable mirror.

There is a diagnostics beamline for improving the electron beam quality in the storage ring (Huang *et al.*, 2007; Huang & Ko, 1998). The interferometer technique has been implemented at this beamline to measure the electron beam size with high resolution.

In this paper, the coherency of the light generated from PLS is investigated using interferograms measured at the diagnostics beamline. A numerical study including the phase calculation of waves from the finite electron beam to the screen is carried out for comparison with measurements. The theory of interference is reviewed in §2. The experimental results are presented in §3, and the numerical study is introduced in §4. Comparisons with experiment and the numerical study are shown in §5, and a summary is provided in §6.

2. Theory of interference

2.1. Temporal coherency

The famous interferometer invented by Michelson shows the change in interferograms in terms of the position of a movable mirror, as shown Fig. 1. The intensity I on the detector can be calculated as

$$I(h) = \left\langle \left| K_1 \tilde{u}(t) + K_2 \tilde{u}[t + \tau(h)] \right|^2 \right\rangle_t, \qquad (1)$$

where τ is the time delay between the two divided beams of light, K_1 and K_2 are the amplitudes of the divided light beams, and $\tilde{u}(t)$ is the complex representation of the light. If K_1 and K_2 are given the same value K, equation (1) becomes (Goodman, 1985; Born & Wolf, 1999)

$$I(\tau) = 2K^2 I_0\big[1 + \big|\tilde{\gamma}(\tau)\big| \cos(2\pi\bar{\nu}\tau + \delta)\big]. \quad (2)$$

In the above equation, I_0 is the intensity without interference as given by $\big|\tilde{u}(t)\big|^2$, $\tilde{\gamma}$ is the complex degree of temporal coherency, $\bar{\nu}$ is the central frequency of the light, and δ is the phase of the interferogram. As we can see from (2), the intensity on the screen will be oscillated by changing the position of the movable mirror.

From the oscillation pattern, we can calculate the temporal coherency, *i.e.* the degree of correlation between the two divided light beams with a certain time delay. The oscillation pattern shows an envelope from which we can quantify the oscillation, named by the visibility V,

$$V = \frac{I_{\max} - I_{\min}}{I_{\max} + I_{\min}} = \big|\gamma(\tau)\big|. \quad (3)$$

There are two assumptions in interference theory for temporal coherence. One is that the radiating source has no finite size. The other is that radiation with different frequency from the same source is a totally random process. The complex degree of temporal coherency $\tilde{\gamma}$ of the light can be calculated from the correlation function of the complex signal function $\tilde{u}$. From the Wiener–Khinchin theorem of the theory of a stationary random process (Wiener, 1930; Khintchine, 1934), the relation between the complex degree of coherency and the power spectrum density is derived as (Born & Wolf, 1999)

$$\tilde{u}(t) = \int_{-\infty}^{+\infty} \tilde{c}(\omega) \exp(i\omega\tau)\, \mathrm{d}\omega, \quad (4)$$

$$\tilde{\gamma}[\tau(h)] = \big\langle \tilde{u}[t + \tau(h)]\tilde{u}^*(t)\big\rangle = \int_0^{+\infty} 4P(\omega) \exp[i\omega\tau(h)]\, \mathrm{d}\omega. \quad (5)$$

Here, ω is the angular frequency of each Fourier component, $\tilde{c}(\omega)$ is the Fourier transform of the complex signal function $\tilde{u}(t)$, and τ is the time delay between the two divided light beams and is given by $2h/c$. From (5), the complex degree of temporal coherency is revealed as the one-side Fourier transform of the power spectral density $P(\omega)$ of the complex signal function.

2.2. Spatial coherency

There are also two important assumptions in interference theory for spatial coherence. One is that all infinitesimal parts of the finite-size light source are assumed to be statistically independent which means there are no correlations between individual infinitesimal parts. The other assumption is that the light from the infinitesimal part has a very narrow spectral bandwidth, which is called quasi-monochromatic light (Goodman, 1985). With Young's interferometer, as shown in Fig. 2, the degree of correlation between two points in a wavefront can be investigated. The degree of correlation is called the spatial coherency of the light. Using the interferometer, we can measure an interference pattern constructed of two waves passing through two slits,

$$I(P) = \left\langle \left| K_1 \tilde{u}\Big(S_1, t - \frac{r_1}{c}\Big) + K_2 \tilde{u}\Big(S_2, t - \frac{r_2}{c}\Big)\right|^2 \right\rangle_t, \quad (6)$$

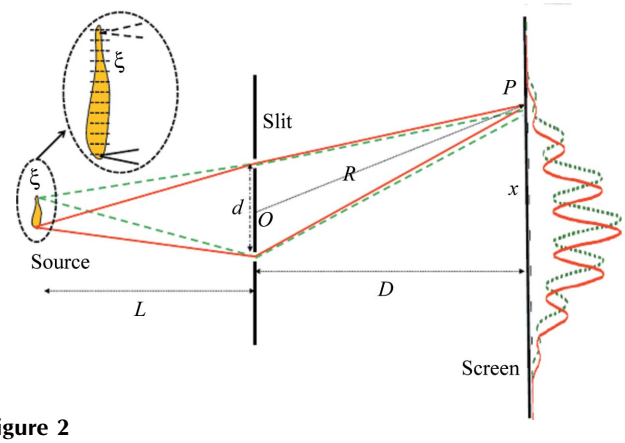

Figure 2
Configuration of the interference with a finite light source. The point O is defined as the centre of the slits. d is the distance between the two square apertures. R is the distance between points O and P on the screen. L is the distance between the source and the diffracting mask. D is the distance from the diffracting mask to the detection screen.

where P is a point on the screen in Fig. 2, S_1 and S_2 are the representations of the two slits, and r_1 and r_2 are the distances from the two slits to the point P. If K_1 and K_2 are given by the same value K, the evaluation of (6) reads

$$I(P) = 2K^2 I_0\Big[1 + \Big|\tilde{\gamma}\Big(\frac{r_2 - r_1}{c}\Big)\Big| \cos\Big(2\pi\bar{\nu}\ \frac{r_2 - r_1}{c} + \delta\Big)\Big]. \quad (7)$$

In the above equation, I_0 is the intensity without interference as given by $|\tilde{u}(t)|^2$, $\tilde{\gamma}$ is the complex degree of spatial coherency, $\bar{\nu}$ is the central frequency of the light, c is the speed of the light in air, and δ is the phase of the interferogram. Along the screen, the intensity will be oscillated by a change in distance d of the slits, because a change in d causes a variation of $(r_2 - r_1)$ in (7). From the oscillation pattern, we can calculate the spatial coherency, *i.e.* the degree of correlation between the two light beams through the slits. The visibility is given by

$$V = \frac{I_{\max} - I_{\min}}{I_{\max} + I_{\min}} = \Big|\tilde{\gamma}\Big(\frac{r_2 - r_1}{c}\Big)\Big|. \quad (8)$$

The spatial coherency of the light from a finite-size source can be estimated from the van Cittert–Zernike theorem as shown (van Cittert, 1934; Zernike, 1938),

$$\tilde{u}(P_1, t) = \int_\sigma \tilde{A}_{\xi 1}\, \frac{\exp\big\{i\big[2\pi\bar{\nu}\big(t - R_{\xi 1}/c\big)\big]\big\}}{R_{\xi 1}}\, \mathrm{d}\xi, \quad (9)$$

$$\gamma_{12}(d) = \big\langle \tilde{u}(P_1, t)\tilde{u}^*(P_2, t)\big\rangle = \int_\sigma I(\xi)\, \frac{\exp\big[i\big(2\pi\bar{\nu}\big\{\big[R_{\xi 1}(d) - R_{\xi 2}(d)\big]/c\big\}\big)\big]}{R_{\xi 1} R_{\xi 2}}\, \mathrm{d}\xi. \quad (10)$$

In the above equations, P_1 and P_2 are the slit positions, ξ is the position of the infinitesimal light source, $\tilde{A}$ is the amplitude of the radiation from the infinitesimal source, $R_{\xi i}$ is the distance from the infinitesimal source to the slit i, $\bar{\nu}$ is the central frequency of the light, and c is the speed of light in air. Let Y_1 and Y_2 be the coordinates of the slit positions P_1 and P_2. We also set

$$p = (Y_1 - Y_2)/L, \tag{11}$$

$$\psi = k\left(Y_1^2 - Y_2^2\right)/2L. \tag{12}$$

Then, (10) is reduced to

$$\gamma_{12}(d) = \exp(i\psi) \int_{\sigma} I(\xi) \exp(-ikp\xi)\, \mathrm{d}\xi, \tag{13}$$

where the wavenumber k equals $2\pi/\lambda$, and L is the distance between the source and the slit. From (13), the complex degree of spatial coherency is revealed as the Fourier transform of the intensity distribution I of the light source.

The spatial variable ξ of the light source distribution in the spatial coherency has the same role as the frequency ν in the power spectral density for the temporal coherency of the light. The time delay between two wavefronts is changed by the distance d between two slits in Young's interferometer and by the distance h in the Michelson interferometer. Each infinitesimal part of the source radiates light with each initial phase and a finite spectral width in nature. However, the wavefront generated from the collection of the infinitesimal parts shows some correlation at certain distances in a wavefront, and is known as partially coherent light. The spatial coherency is a statistical effect of the source distribution, not a property of each infinitesimal part.

3. Experiment

A schematic drawing of the interferometer at beamline 1B1 of PLS is shown in Fig. 3. The radiation generated from the electron beam in the storage ring propagates to the end of the beamline. There are three optical mirrors which reflect only visible light in the transport path of the radiation to the interferometer. A commercial band-pass filter is used between the slit and the detector in the interferometer. The FWHM bandwidth of the optical band-pass filter is 10 nm. In the experiment, 650 nm is selected by the band-pass filter in the interferometer for producing the interferograms. A focusing lens is used to overlap two light beams passing through each slit in the CCD plane. The measured interferogram is shown in Fig. 4 (diamonds). In the measurement, a diffracting mask with two square apertures is used, and the width and length of the apertures are both 3 mm. The distance L between the source and the slit is 24.5 m, and the distance d between the two apertures is 1.3 cm. To extract the source distribution information from the interferogram, we need to compare the measured result with a theoretical model. The formula for an interferogram with a uniformly distributed source and two rectangular apertures is proposed here as follows,

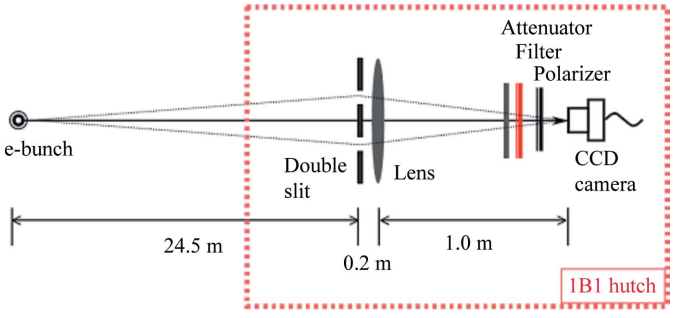

Figure 3
Schematic drawing of beamline 1B1 at PLS.

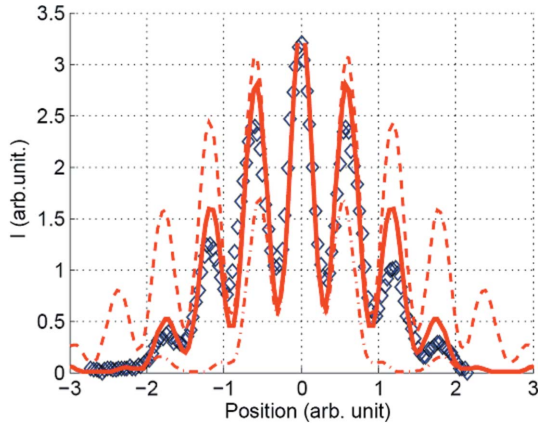

Figure 4
Measured interferogram (diamonds) at PLS and the theory (lines). The solid line is plotted with a = 1.5 mm, the dashed line with a = 1 mm and the dash-dotted line with a = 3 mm.

$$I = 2\left[\frac{\sin(u)}{u}\right]^2\left[1 + \left|\frac{2J_1(v)}{v}\right|\cos(\delta)\right], \tag{14}$$

with

$$u = kax/R, \qquad v = k\xi_{\max}d/L, \qquad \delta = kdx/R,$$

where the wavenumber k is $2\pi/\lambda$, a is the half width of the square aperture, R is the distance between the centre (O) of the slits and a point (P) on the screen, x is the distance of the observation point from the screen centre, $\xi_{\max}$ is the size of the uniformly distributed source, L is the distance between the source and the diffracting mask, and d is the distance between the square apertures.

The solid line in Fig. 4 shows the theoretical prediction of (14) for the uniformly distributed source from $\xi = -336$ µm to $\xi = 336$ µm. To determine the effective half aperture width a for the theory in (14), three lines are plotted using (14) in Fig. 4 with three different values of a. The dashed line in Fig. 4 is plotted for a = 1 mm, the dashed-dot line is for a = 3 mm and the solid line is for a = 1.5 mm. As may be seen, the experimental result is well matched for a = 1.5 mm.

4. Numerical study and analysis for spatial coherency

The electron beam in the storage ring is thought to be a Gaussian distribution (Naito & Mitsuhashi, 2006). However, equation (14), derived for a uniformly distributed source, also gives a good agreement with the experimental result obtained at PLS. To determine the distribution of the electron beam, numerical models of the electron beam are reported in this section. The configuration for the interference with a finite-size light source is given in Fig. 2. As shown in the inset of the figure, the light source can be thought of as a collection of many infinitesimal parts, which all radiate statistically independently. Each source will form its own interferogram; they

do not interfere at all. Thus, the final interferogram should be summed in terms of its intensity, not its amplitude. The intensity is always calculated as the square of the amplitude of the light. For the numerical study of the interferogram, the intensity on the screen should be calculated with the consideration of all phase changes owing to the path difference from the infinitesimal fragment of the light source to a point P on the screen as given by

$$I_\xi(x) = \Big| \sum_\zeta \exp\Big(2\pi\Big\{\big[(\xi-\zeta)^2 + L^2\big]^{1/2} + \big[(x-\zeta)^2 + D^2\big]^{1/2}\Big\}/\lambda\Big)\Big|^2, \quad (15)$$

where x is a point on the screen, ξ is the variable for an infinitesimal fragment in the light source, ζ is the virtual point in the finite size slit, L is the distance between the slit and the source, D is the distance between the slit and the screen, and λ is the wavelength of the light. In this numerical study, the distance L between the source and the slit is 24.5 m, the slit distance d is set to be 1.3 cm, the slit aperture a is 1.5 mm, and the distance D between the slit and screen is 12 km. For short distances $D < 12$ km in the numerical study, the diffraction patterns from each slit do not overlap well on the screen. In the theory, this distance is assumed to be an infinitely long distance (Born & Wolf, 1999). In the experiment, a focusing lens is needed to realise this infinitely long distance and make the two light beams from the two slits overlap within a finite distance in the beamline, as shown in Fig. 3.

The intensities with infinitesimal light sources should be summed because all infinitesimal fragments of the source are statistically independent. For example, there is no physical reason why the radiation from an electron in the electron beam circulating around a storage ring should be correlated with the radiation from another electron. Thus, the final intensity can be calculated as

$$I(X) = \sum_\xi I_\xi(X). \quad (16)$$

Final interferograms using 650 nm wavelength light generated from a Gaussian distribution source and from a uniform distribution source are shown in Fig. 5. Dots in Fig. 5 represents the result with the Gaussian source, and circles show the uniformly distributed source. The solid line is the same as in Fig. 4. In the inset of Fig. 5, the two source distributions used in this numerical study are shown, with the Gaussian distribution with a standard deviation of σ = 210 µm (dots), and the uniformly distributed source from x = −336 µm to x = 336 µm (solid line). For both source distributions, the theory from (14) is quite well matched with the interferograms from the numerical models. An interferogram obtained from a source with a Gaussian distribution of standard deviation σ is similar to that obtained by a uniformly distributed source of 3.2σ FWHM. As shown in Fig. 5, two different radiation source shapes give almost the same interferogram, and it is difficult to identify the shape of the source from one interferogram taken at only a double slit with separation d. In the next section, we will demonstrate a method of identifying the source shape from several measurements with several double slits with variable d.

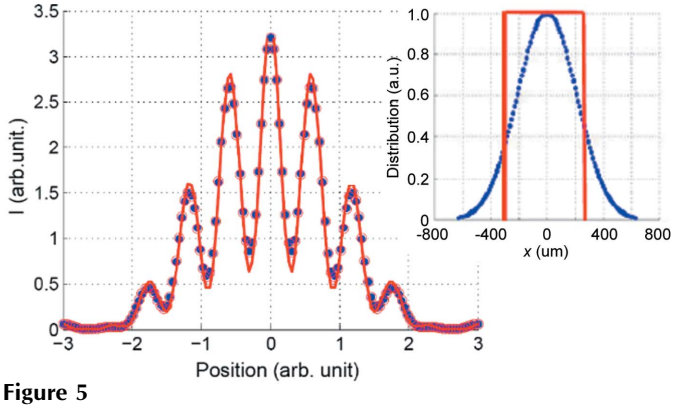

Figure 5
Interferograms obtained using the numerical model with Gaussian distribution (dots) and uniform distribution (circles). The theory of the interferogram is plotted with the solid line using equation (14). L = 24.5 m, D = 12 km, d = 1.3 cm. The half slit width a is 1.5 mm. The inset shows the source distributions. The standard deviation of the Gaussian source distribution (dots) is 210 µm and the region from x = −630 µm to x = 630 µm is used in this numerical study. The uniformly distributed source (solid line) has a FWHM of 672 µm.

5. Spatial coherency and beam size

5.1. Spatial coherency of synchrotron radiation at PAL

To investigate the spatial coherency of the light, the visibility is measured using several diffracting masks with different aperture distance d and the result is represented in Fig. 6 (diamonds). The results obtained with the numerical models for the visibility in terms of the distance d are also shown in Fig. 6. The visibility with a Gaussian distribution is represented by dots and that with the uniformly distributed source by circles. All parameters except d in the numerical study are the same as in Fig. 5. The coherency of the light from the Gaussian distribution of the source shows a different behaviour from the uniformly distributed source as shown in

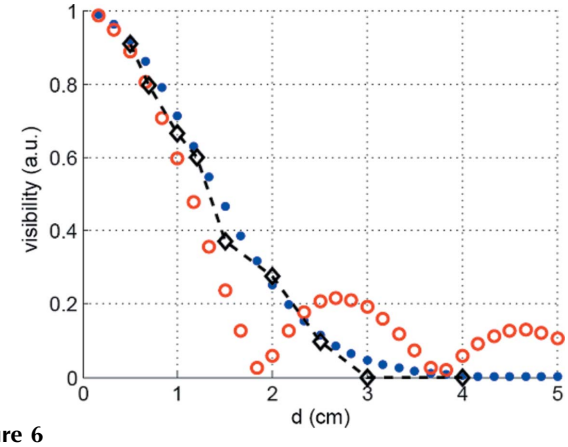

Figure 6
Visibility *versus* d. The wavelength of light is 650 nm. Experimental results are represented by diamonds. Results are shown from the numerical study for the Gaussian (dots) and uniform distributions (circles).

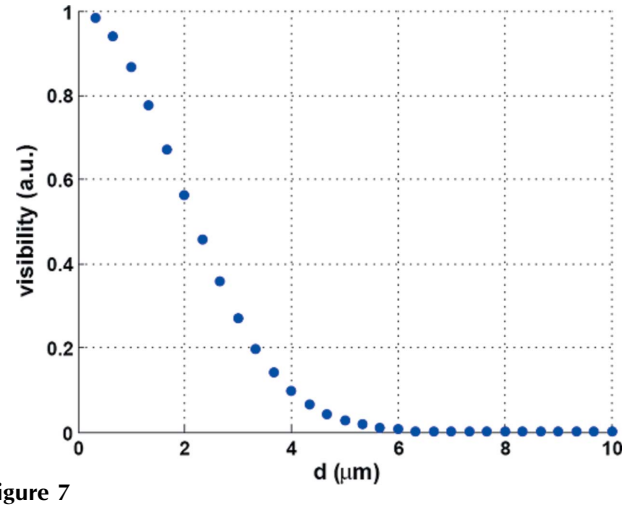

Figure 7
Visibility *versus d*. The wavelength of light is 0.1 nm. Results for the Gaussian distribution with a standard deviation of 210 μm (dots). All simulation parameters are the same as in Fig. 5.

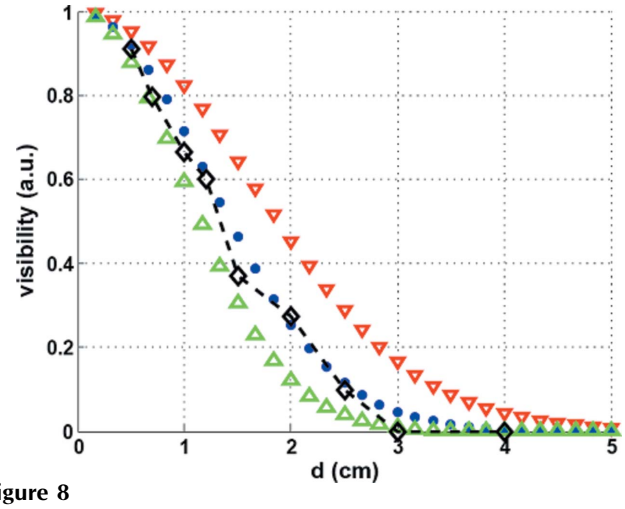

Figure 8
Results for the Gaussian distribution with different standard deviations: 160 μm (inverse triangles), 210 μm (dots) and 260 μm (triangles). All simulation parameters are the same as in Fig. 5.

Fig. 6. The uniformly distributed source shows a bouncing behaviour of the visibility (Born & Wolf, 1999). The measured visibility shows no bouncing behaviour. Even though the uniformly distributed source explains the interference pattern well, the d dependence in the visibility rules out the uniformly distributed source. The spatial coherency length is defined by the slit distance with a visibility value of 0.88 (Born & Wolf, 1999). In Fig. 6, the spatial coherency length of 650 nm light at PLS is obtained as 0.57 cm. For an X-ray beam, the direct measurement of the spatial coherence length is difficult because the order of the length is smaller than micrometres. The spatial coherency of X-rays can be predicted using the code used in this study. In Fig. 7, the spatial coherency of 0.1 nm X-rays is predicted to be 0.88 μm by the same numerical model.

5.2. Evaluation of beam size

The remaining issue is to determine the standard deviation σ of the Gaussian distribution. As shown in Fig. 8, the behaviour of the visibility for different standard deviations of Gaussian distribution sources is different. Results for Gaussian distributions are presented for different standard deviations of 160 μm (inverse triangles), of 210 μm (dots) and of 260 μm (triangles). The visibility in Fig. 8 for a larger source decreases faster with the increase in the distance d. The measured visibility of the interferogram is well matched with the numerical result obtained with a Gaussian distribution with a standard deviation of 210 μm. In conclusion, the electron source distribution at PLS is revealed as a Gaussian distribution with a standard deviation of 210 μm.

6. Summary

The theory of interference is reviewed in order to understand the temporal coherency and the spatial coherency of the light generated from a collection of independent infinitesimal sources. From the measurement results and numerical study, the electron beam at PLS is revealed to be a Gaussian distribution with a standard deviation of 210 μm. The spatial coherency length of 650 nm light at PLS is measured to be 0.57 cm; that of 0.1 nm light is predicted to be 0.88 μm.

This work was supported by a Korea Science and Engineering Foundation (KOSEF) grant funded by the Korea government (Ministry of Education Science and Technology) (No. R0A-2008-000-20013-0). We give great thanks to Dr Sung Ju Park at Pohang Accelerator Laboratory for his help and many discussions.

References

Born, M. & Wolf, E. (1999). *Principles of Optics*, 7th ed. (extended), ch. 10. Cambridge University Press.
Cittert, P. H. van (1934). *Physica*, **1**, 201.
Fisher, A. S., Bong, E. L., Holtzapple, R. L. & Petree, M. (2001). *Proceedings of PAC 2001*, Chicago, USA, p. 547.
Flanagan J. W., Hiramatsu, S. & Mitsuhashi, T. (2000). *Proceedings of EPAC 2000*, Vienna, Austria, pp. 1714–1716.
Goodman, J. W. (1985). *Statistical Optics*, ch. 5. New York: John Wiley and Sons.
Huang, J. Y., Choi, H. J., Kim, C. B. & Han, Y. J. (2007). Report PAL-PUB-2007-004. Pohang Accelerator Laboratory, Pohang University of Science and Technology, Pohang, Republic of Korea.
Huang, J. Y. & Ko, I. S. (1998). *J. Synchrotron Rad.* **5**, 642–644.
Khintchine, A. (1934). *Math. Ann.* **109**, 604.
Masaki, M. & Takano, S. (2003). *J. Synchrotron Rad.* **10**, 295–302.
Mitsuhashi, T. (1999). *Proceedings of the Joint US–CERN–Japan–Russia School on Particle Accelerator Beam Measurements*, pp. 399–427. Singapore: World Scientific Publishing.
Naito, T. & Mitsuhashi, T. (2006). *Phys. Rev. ST Accel. Beams*, **9**, 122802.
Sakai, I., Yamamoto, Y., Mitsuhashi, T., Amano, D. & Iwasaki, H. (2000). *Rev. Sci. Instrum.* **71**, 1264.
Wiener, N. (1930). *Acta Math.* **55**, 117.
Zernike, F. (1938). *Physica*, **5**, 785.